TURBULENT BUBBLY FLOW IN A VERTICAL PIPE COMPUTED BY AN EDDY-RESOLVING REYNOLDS STRESS MODEL

M. Ullrich, R. Maduta and S. Jakirlić*

Institute of Fluid Mechanics and Aerodynamics,
Technische Universität Darmstadt,
Alarich-Weiss-Str. 10, 64287 Darmstadt, Germany
mullrich@sla.tu-darmstadt.de

Abstract

Turbulent incompressible bubbly flow in a vertical pipe in a Reynolds number range is studied computationally by using second-moment closure models. A corresponding instability sensitive eddy-resolving Reynolds stress model is applied in addition to the conventional Reynolds averaged Navier-Stokes approach. The two-phase flow computations are performed by utilizing an Eulerian two-fluid model. The numerical results are compared with available experimental data and data from Direct Numerical Simulation. The implementations of the described models and the computations are done in the numerical code OpenFOAM®.

1 Introduction

Turbulent bubbly flows are encountered in many industrially relevant applications, such as chemical industries or nuclear safety engineering. A commonly used approach to model two-phase flows is the Eulerian two-fluid model by Ishii and Hibiki (2011), which requires closure models for the interfacial momentum transfer and the Reynolds stress tensor in both phases. Modeling of the Reynolds stress tensor in dispersed gas-liquid multiphase flows is still an open field of research. This is due to the complex interactions between the shear induced turbulence of the underlying flow and the modification of the turbulent quantities by the dispersed bubbles. Due to the lack of realisable data through experiments or Direct Numerical Simulation (DNS), which would allow a much more detailed modelling studies, the most common way to account for the turbulence in multiphase flows is to use coventional incompressible single-phase turbulence models, mainly eddy viscosity models, and to extend these models by additional source terms to consider the influence of the bubbles on the turbulent quantities.

A different approach is followed in the present work, where we investigate adiabatic disperse gas-liquid turbulent flows in a vertical pipe in a Reynolds number range, but by using a near-wall second-moment closure model due to Jakirlić and Maduta (2013) to model the Reynolds stress tensor of the liquid phase capable of capturing the anisotropy properties. A recent work where similiar cases are analyzed by utilizing an eddy viscosity model and the above mentioned modifications can be found in Rzehak and Krepper (2013). So far only few investigations have been done by using Reynolds stress models (RSM) up to now. For the case of a bubbly flow in a vertical pipe, Bertodano et al. (1990) used a high-Reynolds number RSM to evaluate the effect of the Reynolds stresses on the lateral pressure gradient and thereby the influence of the turbulence on the radial void fraction profile. This approach is continued here with the aim to avoid any lateral models for the interfacial momentum transfer as far as it is possible for the resulting fully developed two-phase flow equations. These computations represent a prelimanary work. In the next step a version of the length scale-supplying equation extended appropriately in accordance with the Scale-Adaptive Simulation (SAS) proposal of Menter and Egorov (2010) is solved in conjunction with the RSM-equations, to obtain an instability sensitive Reynolds stress model (IS-RSM). Such a modified length scale supplying equation enables the fluctuating turbulent field to be developed.

This work is therefore split up into two parts. In a first step, the incompressible turbulent single-phase flows in a pipe are computed via the Reynolds stress model of Jakirlić and Maduta (2014) and the associated IS-RSM over a Reynolds number range. These results are compared with the experimental data from Hosokawa and Tomiyama (2010) and DNS data from Khoury et al. (2013) and Wu et al. (2012). This is the first investigation of a pipe geometry with the present IS-RSM. In a second step, a turbulent bubbly pipe flow from Hosokawa and Tomiyama (2010) is investigated, by incorporating the previously described models into the Eulerian two-fluid framework. The influence of the turbulent stresses on the radial distribution of the gas volume fraction should be hereby analyzed.

*Present address Outotec GmbH, Ludwig-Erhard-Strasse 21, D-61440 Oberursel Germany

2 Eulerian two-fluid model

The following formulation of the Eulerian two-fluid model, in cartesian coordinates, taken from Ishii and Hibiki (2011), is used for an adiabatic, incompressible flow without phase change consisting of the continuity equation

$$\frac{\partial \alpha_\varphi}{\partial t} + \frac{\partial(\alpha_\varphi U_j^\varphi)}{\partial x_j} = 0 \tag{1}$$

and the momentum equation

$$\frac{\partial(\alpha_\varphi U_i^\varphi)}{\partial t} + \frac{\partial(\alpha_\varphi U_j^\varphi U_i^\varphi)}{\partial x_j} = -\frac{\alpha_\varphi}{\rho_\varphi}\frac{\partial \overline{p}}{\partial x_i} + \alpha_\varphi g_i + \frac{\partial}{\partial x_j}\left[\alpha_\varphi \nu_\varphi \left(\frac{\partial U_i^\varphi}{\partial x_j} + \frac{\partial U_j^\varphi}{\partial x_i}\right)\right] + \frac{M_i^\varphi}{\rho_\varphi} + \frac{\partial \alpha_\varphi R_{ij}^\varphi}{\partial x_j} \tag{2}$$

with φ denoting either the gas phase $\varphi \equiv G$ or the liquid phase $\varphi \equiv L$: $\Sigma_\varphi \alpha_\varphi = 1$. The conditional averaged velocity and pressure, the volume fraction, viscosity, density and gravitational vector are denoted by U_i^φ, $\overline{p}$, α_φ, ν_φ, ρ_φ and g_i. This system of partial differential equations needs appropiate closure models for the interfacial momentum transfer term M_i^φ and the Reynolds stress tensor $R_{ij}^\varphi$of both phases. The modelling of the interfacial momentum transfer term with $M_i^{\mathrm{L}} = -M_i^{\mathrm{G}}$, is mainly based on considering different interfacial forces which are derived from experimental observations and theoretical thoughts. The drag and virtual mass forces are commonly considered for nearly all relevant test cases because of their important influence on the velocity in the flow direction. In this work the drag force is modelled via the Tomiyama et al. (1995) drag correlation and the virtual mass force is modelled with the coefficient $\mathrm{C_{VM}}$ taking the standard value of 0.5.

Other forces which mainly act in the lateral direction, like the lift, wall lubrication and turbulent dispersion force, see Ishii and Hibiki (2011) for a summary, are usually referred to be responsible for the radial distribution of the void fraction in a vertical pipe flow. This is highly arguable, since their origin and physical rationale is mostly unclear and their influence strongly affected by the combination between themself and the used turbulence model. By taking a look at the radial momentum equations in cylindrical coordinates for a fully-developed bubbly turbulent pipe flow in a conventional Reynolds averaged Navier-Stokes (RANS) sense, by neglecting the turbulence in the gas phase, the equations simpflies to the following forms pertinent to the gas phase

$$\frac{\alpha_{\mathrm{G}}}{\rho_{\mathrm{G}}}\frac{\partial \overline{p}}{\partial r} = -\frac{M_r^{\mathrm{L}}}{\rho_{\mathrm{G}}} \tag{3}$$

and to the liquid phase

$$\frac{\alpha_{\mathrm{L}}}{\rho_{\mathrm{L}}}\frac{\partial \overline{p}}{\partial r} = \frac{M_r^{\mathrm{L}}}{\rho_{\mathrm{L}}} - \frac{d\alpha_{\mathrm{L}} R_{rr}^{\mathrm{L}}}{dr} + \frac{\alpha_{\mathrm{L}}}{r}\left(R_{\varphi\varphi}^{\mathrm{L}} - R_{rr}^{\mathrm{L}}\right) \tag{4}$$

with M_r^{L} being the radial component of the interfacial momentum transfer term, R_{rr}^L the radial stress component and $R_{\varphi\varphi}^L$ the azimuthal stress component. By analyzing Eq. (4) it becomes clear that the turbulence plays the same role as in single-phase flows, where the radial pressure gradient is induced by the turbulence. The influence on α_{G} becomes more clear by eliminating the pressure gradient from Eq. (4) by Eq. (3), leading to

$$\alpha_{\mathrm{G}}\frac{d\alpha_{\mathrm{G}}}{dr} = \frac{\alpha_{\mathrm{G}}(1-\alpha_{\mathrm{G}})}{R_{rr}^L}\left[\frac{dR_{rr}^L}{dr} - \frac{R_{\varphi\varphi}^L - R_{rr}^L}{r}\right] - \frac{M_r^{\mathrm{L}}}{\rho_{\mathrm{L}} R_{rr}^L} \tag{5}$$

Therefore in a fully developed vertical pipe flow, the distribution of α_{G} depends strongly on the interfacial forces in radial direction and the turbulent quantities in the liquid phase. This equation has been used by Drew and Lahey (1982) in a similiar form and solved analytically, by neglecting the interfacial forces and modelling the turbulence in the liquid phase via a mixing length model. As mentioned by Bertodano et al. (1990) neglecting interfacial forces in radial direction forces the radial pressure gradient to become zero in areas where α_G is non zero, because of Eq. (3) and thereby interact with the turbulence structure through Eq. (4). Because of that the choice of the interfacial momentum transfer term does not only influence the radial distribution of α_{G} but also interacts with the turbulent quantities. To avoid $\partial p/\partial r$ becoming zero in areas where α_{G} exist, a specific model by Drew and Lahey (1987) for the so-called turbulent dispersion force is choosen

$$M_r^{\mathrm{L}} = C_{\mathrm{TD}}\rho_{\mathrm{L}} k \frac{d\alpha_{\mathrm{G}}}{dr} \tag{6}$$

with the turbulent dispersion force coefficient C_{TD}, set presently to unity, and the turbulent kinetic energy of the liquid phase k. This model has the advantage that it is easy to implement and is also related to the turbulence of the liquid phase. On the other hand every selection of such a model is controversary, since the question arises whether or not it is valid for the present test case and does it influence the turbulence in an undesirable way.

A proper way to avoid such situations would be the use of an eddy-resolving model, which would lead to a fluctuating velocity field and therefore avoiding the left hand side of Eq. (1) and Eq. (2) to become zero.

3 Turbulence Modeling

To compute the Reynolds stress tensor in the carrier liquid phase the near wall second-moment closure model of Jakirlić and Maduta (2014), based on the model by Jakirlić and Hanjalić (2002), is used. To extend the RSM towards two-phase flow, the volume fraction α_{L} is incorporated straight-forwardly into the

corresponding transport equations leading to the following equation system

$$\frac{D\alpha_{\rm L}R^{\rm L}_{ij}}{Dt} = -\alpha_{\rm L}\left(R^{\rm L}_{ik}\frac{\partial U^{\rm L}_j}{\partial x_k}+R^{\rm L}_{jk}\frac{\partial U^{\rm L}_i}{\partial x_k}\right) +\alpha_{\rm L}\Phi_{ij}+\alpha_{\rm L}\varepsilon^h_{ij}+\frac{1}{2}\mathcal{D}^{\nu}_{ij}+\mathcal{D}^{t}_{ij} \quad (7)$$

with Φ_{ji} representing the pressure strain tensor, $\mathcal{D}^{\nu}_{ij}$ and $\mathcal{D}^{t}_{ij}$ the molecular and turbulent diffusion transport terms (where $\alpha_{\rm L}$ is also included) and ε^h_{ij} the homogeneous part of the stress dissipation tensor. The detailed specification of these model terms can be found in Jakirlić and Maduta (2014). The overscript L has been omitted here, since all turbulent quantities are related to the carrier liquid phase. Contrary to the RSM model by Jakirlić and Hanjalić (2002) utilizes the present model the transport equation for the homogeneous part of the inverse turbulent time scale ω_h as a supplying length scale-variable. The corresponding transport equation for ω_h has been directly derived from the equation governing the homogeneous fraction of the total viscous dissipation rate ε_h and is modelled in a term-by-term manner leading to

$$\frac{D\alpha_{\rm L}\omega_h}{Dt} = \frac{1}{2}\mathcal{D}^{\nu}_{\omega_h}+\mathcal{D}^{t}_{\omega_h} +\alpha_{\rm L}\left(C_{\omega_h,1}\frac{\omega_h}{k}\mathcal{P}_k+C_{\omega_h,2}\omega_h^2\right) +\frac{2\alpha_{\rm L}}{k}\left(0.55\frac{1}{2}\nu+0.275\frac{\nu_t}{\sigma_\omega}\right)\frac{\partial k}{\partial x_k}\frac{\partial \omega_h}{\partial x_k} \quad (8)$$

with $\mathcal{P}_k = -R^{\rm L}_{ij}\partial U^{\rm L}_i/\partial x_j$ representing the production rate of k. The detailed specification of the unclosed model terms can be found in Jakirlić and Maduta (2014). Additional source terms due to bubble induced effects are not included into these transport equation, since the focus of this work segment lies on the effects of capturing the anisotropy of the Reynolds stress tensor rather than the effects of additional source terms.

This RSM is used preliminary to compute the flow in a two dimensional axis-symmetric pipe for both single-phase and two-phase flow. In the next step a version of the ω_h-equation extended appropriately in accordance with the SAS proposal by Menter and Egorov (2010) is solved in conjunction with the RSM-equations. The key term in this eddy-resolving model resembles a production term defined in terms of the von Karman length scale containing second derivative of the velocity field, being capable of capturing the vortex size variability. Such a modified ω_h-equation enables the fluctuating turbulent field to be developed. The corresponding ω_h-equation solved in the framework of the instability-sensitive-RSM (IS-RSM) model reads:

$$\left(\frac{D\alpha_{\rm L}\omega_h}{Dt}\right)_{\rm SAS} = \frac{D\alpha_{\rm L}\omega_h}{Dt}+\alpha_{\rm L}P_{\rm SAS} \quad (9)$$

with $P_{\rm SAS}$ taking the form adjusted appropriately to the underlying RSM (see Maduta (2013)):

$$P_{\rm SAS} = 0.004\max\left(2.3713\kappa S^2\left(\frac{L}{L_{\rm vK}}\right)^{\frac{1}{2}}-8T_2,0\right),$$
$$T_2 = 3k\max\left(\frac{1}{\omega_h\omega_h}\frac{\partial\omega_h}{\partial x_j}\frac{\partial\omega_h}{\partial x_j},\frac{1}{k^2}\frac{\partial k}{\partial x_j}\frac{\partial k}{\partial x_j}\right) \quad (10)$$

with $L = k^{1/2}/\omega_h$ representing the turbulent length scale and $L_{\rm vK} = \kappa S/|\nabla^2\mathbf{U}^{\rm L}|$ the von Karman length scale ($S = \sqrt{S^{\rm L}_{ij}S^{\rm L}_{ij}}$). This IS-RSM model has been applied by Maduta and Jakirlić (2012) and Maduta (2013) to various turbulent single-phase flows of different complexity resulting in a very good representation of the mean flow field and associated turbulence.

The turbulence in the bubbly gas phase was neglected, as it was done for the present test case by Hosokawa and Tomiyama (2009).

4 Numerical method

All calculations were performed using the OpenFOAM-2.2.2 computational code utilizing a cell-center-based finite volume method on an unstructured numerical grid. The computations with the RSM, that means in a classical RANS framework, were done on a two dimensional axi-symmetric solution domain. For the single-phase flow computations periodic boundary conditions, with one cell in flow direction, are used to obtain a fully developed flow. An appropiate pressure gradient corresponding to the target bulk Reynolds number was imposed.

These results provide the boundary conditions for the two-phase flow computations at the inlet of the domain regarding the mean liquid velocity and the required turbulent quantities. Block profiles corresponding to the average values were used for $\alpha_{\rm G}$ = 0.033 and the mean gas velocity, in accordance with the case 4 from Hosokawa and Tomiyama (2009). The domain was $160D$ long in mean flow direction, with D being the pipe diameter, to obtain fully developed flow conditions. The experimental results were measured at z/D = 68 after the mixing section and it was assumed that the two-phase flow is fully-developed at that point. The unsteady IS-RSM computations have been done on a fully three dimensional grid, by also using periodic boundary conditions. The wall-next grid point corresponds to $y^+ < 1$ for all present computations. The length of the pipe was $2.5D$. An O-grid, which is shown in Fig. 1, was used for setting up the numerical grid with 80 cells in axial direction, 288 cells in azimuthal direction and 100 cells in radial direction resulting in 1.2 million cells in total. The convective transport term in the equation for the mean liquid velocity is thereby discretized by using a fixed blended scheme with 98 per cent CDS and 2 per cent UDS.

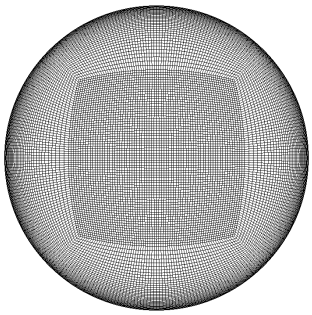

Figure 1: Visualization of the O-grid over a z plane

The temporal discretization is of second order accuracy and a fixed time step is choosen by assuring that the mean Courant number is always below 0.4. The utilized turbulence models were implemented into the so-called twoPhaseEulerFoam solver in OpenFOAM, to carry out the two-phase flow computations. For the two-phase IS-RSM computations a modified pressure gradient corresponding to the flow rate of both phases was applied.

5 Results

The single-phase flow computations with the liquid carrier phase as the working medium are performed for two bulk Reynolds numbers $Re_D = U_b D/\nu_\mathrm{L}$ = 12500 and 25000, with U_b being the bulk liquid velocity, and compared with the experimental data from Hosokawa and Tomiyama (2010). Additionally to these experiments, the DNS data from Khoury et al. (2013) for Re_D = 11900 and Wu et al. (2012) for Re_D = 24580 are used to validate the single-phase flow results. The slight deviation from the experimental Re_D can be neglected. The computed instantaneous velocity fields for the streamwise velocity component U_z^L for the two investigated Reynolds numbers in a single-phase flow are depicted in Fig. 2.

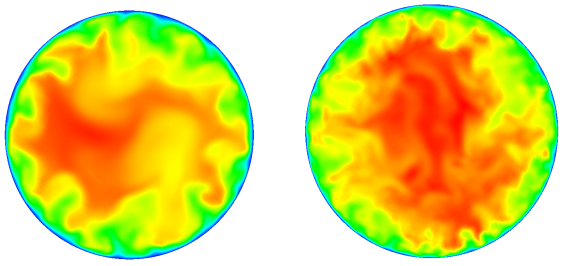

(a) Re_b = 12500 (b) Re_b = 25000

Figure 2: Visualization of turbulent pipe flow over a constant z plane using instantaneous axial velocity component U_z^L

It is shown that the IS-RSM is capable of resolving the turbulence structures in a pipe flow, even when starting with uniformly distributed initial flow fields and no additional artificially imposed fluctuations.

These time-dependent simulations have been averaged over a significant time period of at least 100 flow through times based on the bulk velocity. This results in the mean velocity profile U_m for the single-phase flow computations displayed in Fig. 3 and Fig. 4 exhibiting good agreement with the available DNS data and the reference experiments under the fully-developed flow conditions. There is no significant difference between the reference data and the results obtained with the RSM. Only the results for the higher Reynolds number obtained by the IS-RSM slightly underestimate the reference data in the core region of the flow.

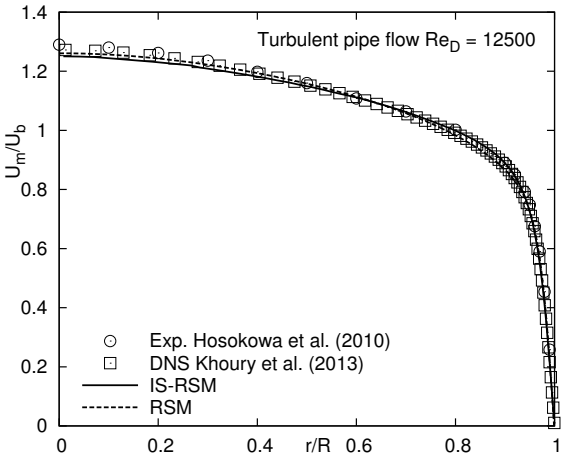

Figure 3: Normalized streamwise velocity

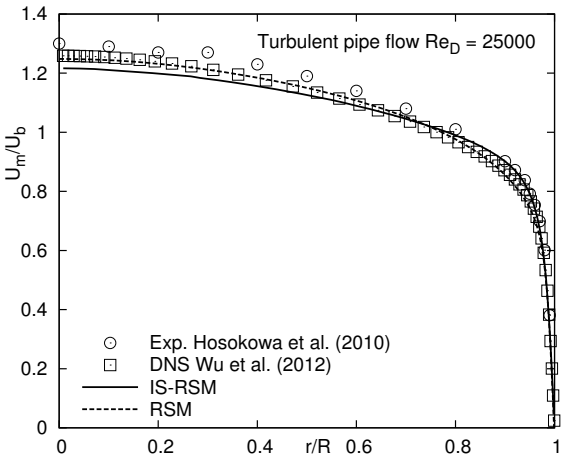

Figure 4: Normalized streamwise velocity

The results for the normalized turbulent intensities $u_i^+ = u_i/U_b$ in Fig. 5 and Fig. 6 show also good agreement with the reference data. While the u_i^+ values computed with the RSM originate only from the modelled Reynolds stress tensor R_{ii}^L, the results computed with the IS-RSM originate from both the mod-

elled part and the time-averaged resolved fluctuations and are calculated via

$$u_i = \sqrt{\overline{\left(U_i^L - \overline{U_i^L}\right)^2} + \overline{R_{ii}^L}} \qquad (11)$$

with no summation over ii. Whereas the RSM show slightly better predictions in the near wall region for Re_D = 11900, the IS-RSM is able to improve the results in the core region of the flow. The overprediction of the Reynolds stress intensities in the region around the symmetry axis pertinent to the steady RSM originates from the use of the Daly and Harlow (1970) turbulent diffusion model. It is well-known that this model formulation is not invariant with respect to the coordinate system transformation. Such a discrepancy vanishes after the turbulence unsteadiness have been reproduced by the IS-RSM.

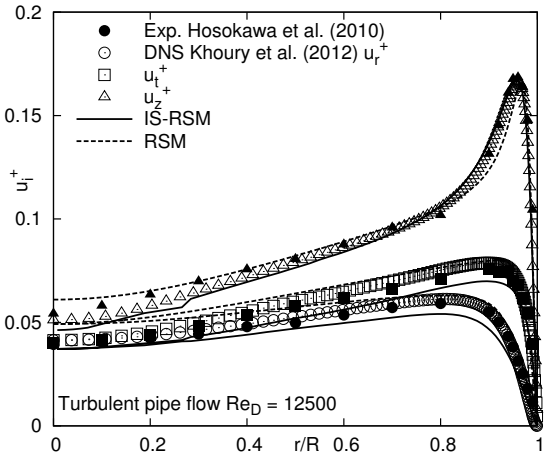

Figure 5: u_i^+ for Re_D = 12500

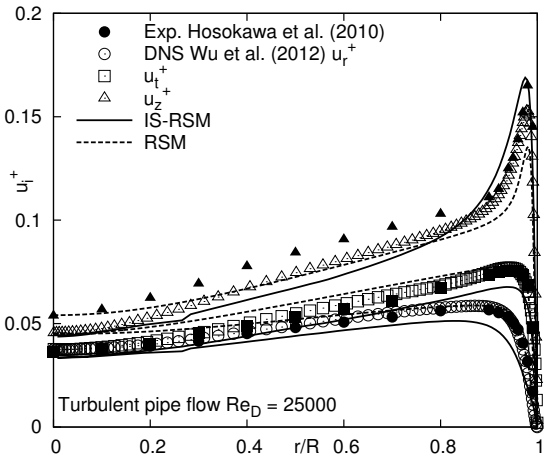

Figure 6: u_i^+ for Re_D = 25000

For Re_D = 25000 the IS-RSM slightly overpredicts the axial stress component u_z^+, while u_r^+ and u_t^+ show the same deviation from the reference data as for Re_D = 12500. This behaviour was also seen by Maduta (2013) for a plane channel flow at Re_τ = 395. The overprediction of u_z^+ is most probably related to an insufficient grid resolution in axial direction.

The calculated radial pressure profiles are compared with the DNS data for the high Re_D in Fig. 7, since the pressure has an essential influence on the radial distribution of the dispersed gas phase. A very good agreement obtained by the present RSM in the near wall region is obvious, being consistent with the good results for the stresses in Fig. 6. On the other hand the specific deviation in the core region is associated with the overprediction of the Reynolds stresses. The IS-RSM leads to slightly improved results in this region.

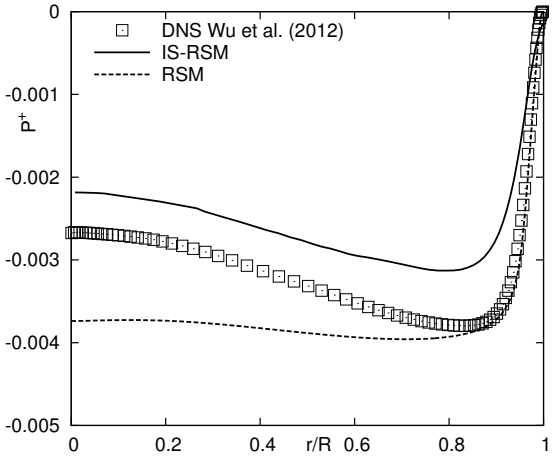

Figure 7: Normalized pressure distribution

The two-phase flow computations were done with an average value of α_G = 0.033 and a superficial liquid velocity corresponding to the previously investigated Reynolds number of Re_D = 25000, with the RSM resulting in the α_G field show in Fig. 8 for different positions z/D in flow-direction. It is shown that the model is capable of correct capturing the accumulation of gas close to the wall. This also valid with respect to the correctly reproduced radial position of the near-wall α_G peak value. The slightly increasing values of α_G in the core region of the flow are related to the underestimated pressure gradient for the baseline single-phase flow. In many computational approaches a so-called wall-lubrication force is to be held responsible for the fact that the bubbles are not touching the wall, but for a near-wall RANS model, which is capable of capturing the increasing pressure close to the wall, the use of such a force can be avoided. On the other hand it is visible that there are still some changes in α_G magnitude in terms of the streamwise postion even after z/D = 160. This uncertainty has to be verified in future works, since a final evaluation can only be done, after

a fully developed flow condition is assured.

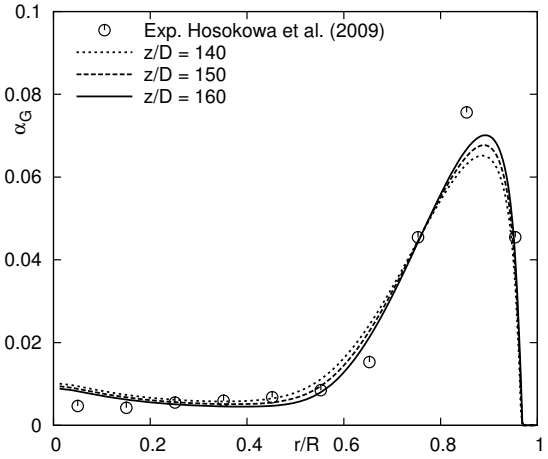

Figure 8: α_{G} distribution for Re_D = 25000 at different position z/D

The computed values for the mean axial relative velocity U_z^r = U_z^{G} - U_z^{L} in axial direction are shown in Fig. 9 for the z/D = 160. The relative velocity is slightly overestimated. This behaviour was also seen by Hosokawa and Tomiyama (2009) for the presently used drag model. A more complex model for the drag force, e.g. the one proposed by Legendre and Magnaudet (1998) could improve the results.

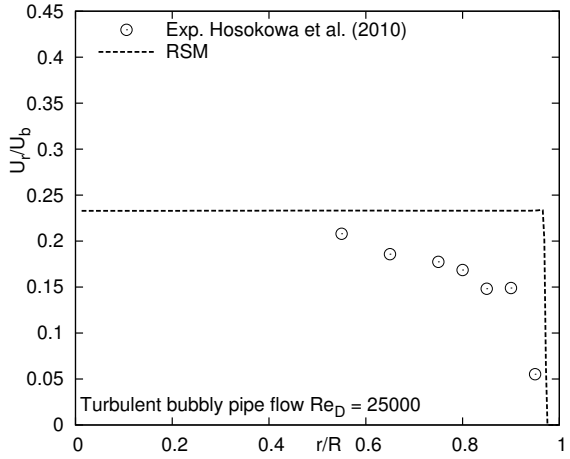

Figure 9: Normalized axial relative velocity

The computed values for the stress components for the two-phase flow are shown in Fig. 10. The RSM is capable to capture the behaviour of the radial and azimuthal turbulent intensities, since this quantities are not essentially influenced by the presence of the disperse phase. The model is not capable to capture the increased peak value of u_z^+. This leads to the conclusion that additional bubble-related source terms in Eq. (7) and Eq. (8), could be necessary to correctly computed this value.

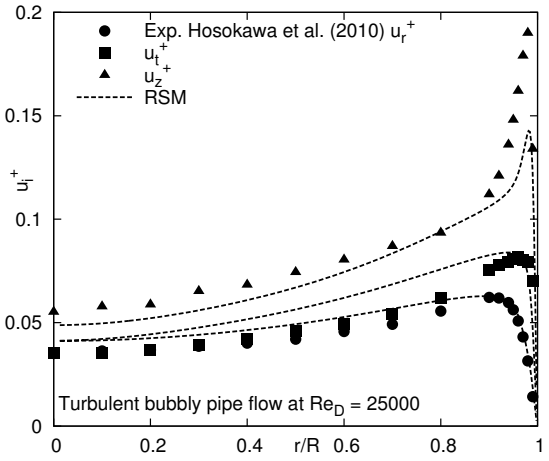

Figure 10: u_i^+ for a bubbly pipe flow at Re_D = 25000

The simulations with the IS-RSM for two-phase flows are still in progress for a few more flow-through times. However as it can be seen in Fig. 11, the IS-RSM is capable of resolving the unsteady nature of the turbulent flow even in this two-phase flow and resulting thereby in the fluctuating fiels of α_{G}, here the red colour denotes a value of α_{G} = 0.4.

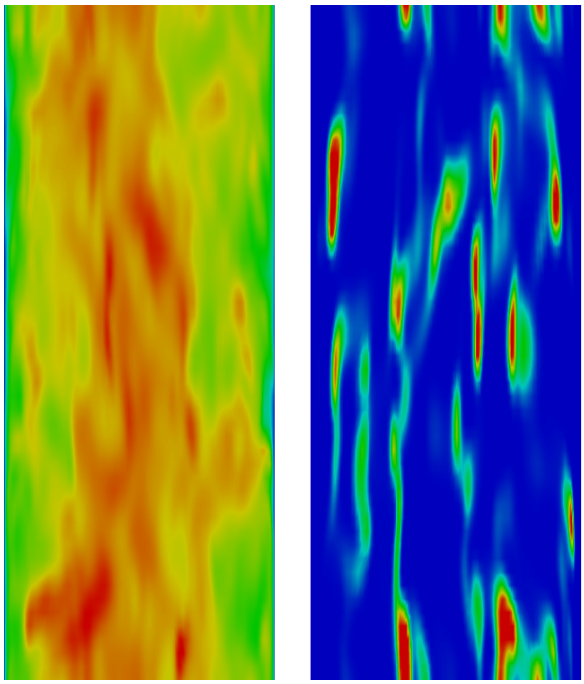

(a) U_z^{L} (b) α_{G}

Figure 11: Visualization of turbulent bubbly pipe flow in the r-φ plane

6 Conclusions

The Reynolds stress models employed in both a conventional steady RANS framework and as an instability-sensitive model in the unsteady RANS framework are used to compute a turbulent bubbly flow in a vertically positioned pipe configuration. For the corresponding single-phase computations both models result in overall good agreement with the available reference data. Especially interesting is the fluctuating turbulence field obtained by the IS-RSM model, which started from the steady flow field with no fluctuations imposed. It is shown that the IS-RSM is capable of resolving the turbulent structures in two-phase flows and thereby a fluctuating field of α_{G}. For the two-phase flow calculation, the coventional RSM yields satisfactory results of the time-averaged flow properties. In a future work, different models for the drag force wil be applied to eventually improve the resulting relative velocities between both phases. The simulations of the bubbly flow by using the instability sensitive RSM are still running for a few more flow-through times.

Acknowledgments

The presented project was funded by the German Federal Ministry of Economic Affairs and Energy (BMWi, project no. 1501417) on basis of a decision by the German Bundestag.

References

Bertodano, M.L. et al. (1990), The Prediction of Two-Phase Turbulence and Phase Distribution Phenomena Using a Reynolds Stress Model, Journals of Fluid Engineering, Vol. 112, pp. 107-113

Daly, B.J. and Harlow F.H. (1970), Transport equations in turbulence, Phys. Fluids., Vol 13, pp. 2634-2649

Drew, D.A. and Lahey, R.T. (1982), Phase distribution mechanisms in turbulent low-quality two-phase flow in a circular pipe, *J. Fluid Mech.*, Vol. 117, pp. 91 -106

Drew, D.A. and Lahey, R.T. (1987), The virtual mass and lift forces on a sphere in a rotating and straining flow, International Journal of Multiphase Flow, Vol. 13, pp. 113-121

Hosokawa, S and Tomiyama, A. (2009), Multi-fluid simulation of turbulent bubbly pipe flows, Chemical Engineering Science, Vol. 64, pp. 5308-5318

Hosokowa, S. and Tomiyama, A. (2010), Effects of bubbles on turbulent flows in vertical channels, ICMF 2010, Tampa, USA

Ishii, M. and Hibiki, T. (2011), Thermo-Fluid dynamics of two-phase flow, second edition, Springer Science

Jakirlić, S. and Hanjalić, K. (2002), A new approach to modelling near-wall turbulence energy and stress dissipation, *J. Fluid Mech.*, Vol. 439, pp. 139-166

Jakirlić, S. and Maduta, R. (2014), On "Steady" RANS Modeling for improved Prediction of Wall-bounded Separation, SciTech 2014, 52nd AIAA Aerospace Sciences Meeting, National Harbor, MD, USA, January 13-17

Khoury, G. K. et al. (2013), Direct numerical Simulation of turbulent pipe flow at moderately high reynolds number, *FTaC*, Vol. 91, pp. 475-495

Legendre, D. and Magnaudet J. (1998), The lift force on a spherical bubble in a viscous linear shear flow, Journal of Fluid Mechanics, Vol. 368, pp. 81-126

Maduta, R. and Jakirlić, S. (2012), An eddy-resolving Reynolds stress transport model for unsteady flow computations, In "Advances in Hybrid RANS-LES Modelling 4", Vol. 117, pp. 77-89

Maduta, R. (2013), An eddy-resolving Reynolds stress model for unsteady flow computations: development and application, PhD Thesis, TU-Darmstadt

Menter, F.R. and Egorov, Y. (2010), The Scale-Adaptive simulation method for unsteady turbulent flow predictions. Part 1: Theory and model description, *FTaC*, Vol. 85, pp. 113-138

Rzehak, R. and Krepper, E. (2013), CFD modeling of bubble-induced turbulence, International Journal of Multiphase Flows, Vol. 55, pp. 138-155

Tomiyama, A. et al. (1995), Drag coefficients of bubbles: 2nd report, drag coefficient for a swarm of bubbley and its applicability to transient flow. Transactions of JSME 61 (588)m 2810-2817 (in Japanese)

Wu, X. et al. (2012), Direct numerical simulation of a 30R long turbulent pipe flow at R^{+}: large- and very large-scale motions, *J. Fluid Mech.*, Vol. 698, pp. 235-281